Available online at www.sciencedirect.com

ScienceDirect

Procedia Computer Science 00 (2022) 1–9

Procedia Computer Science

Abstract

Keywords:

1. Introduction

The Hybird High Order method (HHO) is a discontinuous discretization method, that takes root in the Discontinuous Galerkin method (DG). From the physical standpoint, DG methods ensure the continuity of the flux across interfaces, by seeking the solution element-wise, hence allowing jumps of the potential across elements. They can be seen as a generalization of Finite Volume methods, and are able to capture physically relevant discontinuities without producing spurious oscillations.

The origin of DG methods dates back to the pioneering work of [1], where an hyperbolic formualtion is used to solve the neutron transport equation. The first application of the method to elliptic problems originates in [2] where Nitsche's method [3] is used to weakly impose continuity of the flux across interfaces. In 2002, Hansbo and Larson [4] were the first to consider the Nitsche's classical DG method for nearly incompressible elasticity. They showed, theoretically and numerically, that this method is free from volumetric locking. However, the bilinear form arising from this formulation is not symmetric. A so called interior penalty term has been introduced in [5], leading to the Symmetric Interior Penalty (SIP) DG method. A first study of the method to linear elasticity has been devised by [6], where optimal error estimate has been proved. [7] generalized the Symmetric Interior Penalty method to linear elasticity. period of time, DG methods were proposed for other linear problems in solid mechanics, such as Timoshenko beams [8], Bernoulli-Euler beam and the Poisson-Kirchhoff plate [9, 10] and Reissner-Mindlin plates [11]. In the mid 2000's, the first applications of DG methods to nonlinear elasticity problems was undertaken by [12, 13], and in 2007, Ortner and Süli [14] carried out the a priori error analysis of DG methods for nonlinear elasticity.

DG methods then sollicitated a vigourus interest, mostly in fluid dynamics [15, 16] due to their local conservative property and stability in convection domniated problems. However, except some applications for instance in fracture mechanics using XFEM methods [17, 18], or gradient plasticity [19, 20] DG methods did not break through in computational solid mechanics because of their numerical cost, since nodal unknowns need be duplicated to define local basis functions in each element.

To adress this problem, in the early 2010's, [21, 22] introduced additional faces unknowns on element interfaces for linear elastic problem, hence leading to the hybridization of DG methods, or Hybridizable Discontinuous Galerkin method (HDG). By adding supplementary boundary unknowns, the authors actually allowed to eliminate original cell unknowns by a static condensation process, in order to express the global problem on faces ones only. Extension of HDG methods to non-linear elasticity were first undertaken in [23] and have then fueled intense reaserch works for various applications such as linear and non-linear convection-diffusion problems [24, 25, 26], incompressible stokes flows [26, 27] and non-linear mechanics [28].

In [29, 30], the authors introduced a higher order potential reconstruction operator in the classical HDG formulation for elliptic problems, providing a $h^{k+1}H^1$-norm convergence rate as compared to the ususal h^k-rate. This higher order term coined the name for the so called HHO method. Recent developments of HHO methods in computational mechanics include the incompressible Stokes equations (with possibly large irrotational forces) [31], the incompressible Navier–Stokes equations [32], Biot's consolidation problem [33], and nonlinear elasticity with small deformations [34]

The difference between HHO and HDG methods is twofold: (1) the HHO reconstruction operator replaces the discrete HDG flux (a similar rewriting of an HDG method for nonlinear elastic- ity can be found in [29]), and, more importantly, (2) both HHO and HDG penalize in a least-squares sense the differ- ence between the discrete trace unknown and the trace of the discrete primal unknown (with a possibly mesh-dependent weight), but HHO uses a non-local operator over each mesh cell boundary that delivers one-order higher approximation than just penalizing pointwise the difference as in HDG. Discretization methods for linear and nonlinear elastic- ity have undergone a vigorous development over the last decade. For discontinuous Galerkin (dG) methods, we men- tion in particular [14,26,32] for linear elasticity, and [35,41] for nonlinear elasticity. HDG methods for linear elasticity have been coined in [38] (see also [13] for incompressible Stokes flows), and extensions to nonlinear elasticity can be found in [29,34,37]. Other recent developments in the last few years include, among others, Gradient Schemes for nonlinear elasticity with small deformations [22], the Virtual Element Method (VEM) for linear and nonlinear elasticity with small [3] and finite deformations [8,43], the (low-order) hybrid dG method with conforming traces for nonlinear elasticity [44], the hybridizable weakly conforming Galerkin method with nonconforming traces for linear elasticity [30], the Weak Galerkin method for linear elasticity [42], and the discon- tinuous Petrov–Galerkin method for linear elasticity [7].

Contrary to the standard (*i.e.* the Lagrange) Finite Element method, non-conformal methods (among which the Hybrid High Order one) postulate the discontinuity of the displacement field across elements. Hence, each element is *a priori* free to move independently from others; in order to restore a weak form of continuity on the mesh, a *stabilization* term is computed, to penalize in a least square sense the displacement jump between two neighbouring cells. The displacement jump between elements is exploited to define discrete operators in each element, that provide conservation of physcial properties. Moreover, the Hybrid High Order method is hybrid, hence introducing faces unknowns in addition to the regular cells ones. Morover, cell unknowns are expressed in terms of coefficients in a polynomial basis, that have no physcial meaning, as opposed to the ususal nodal unknowns of Lagrange finite elements. This feature allows to equivalently express shape functions on any generic polygonal element, as opposed to the Lagrange Finite Element method that needs particlaur shape function for each element geometry.

All these differences with the wide spread Lagrange Finite Element method make the Hybrid High Order one more ununderstandable to a computational mechanics public. Discontinuous methods were developed by the mathematical community, such that they are put forward in the literature through a possibly arid way for the computational mechanics reader. Therefore, in the present document, we propose an introduction to these methods, based on mechanical arguments, by considering the ususal continuous framework proper to the standard Finite Element method, and using a limit case to meet the discontinous setting in which lies the HHO method.

In a second part, we propose and devise a Hybrid High Order method for axisymetrical configurations.

2. The Hybrid High Order method

2.1. Description of the model problem

Let $d \in \{1, 2\}$ the euclidean dimension of the cartesian space $\mathbb{R}^d$, and $\mathcal{R}_d$ the euclidean reference frame. Let $\Omega \subset \mathbb{R}^d$ a solid body with boundary $\partial\Omega \subset \mathbb{R}^{d-1}$, that deforms under the volumic load $\boldsymbol{f}_v$. It is subjected to a prescribed displacement $\boldsymbol{u}_d$ on the Dirichlet boundary $\partial\Omega_d$, and to a contact load $\boldsymbol{t}_n$ on the Neumann boundary $\partial\Omega_n$, such that $\partial\Omega = \partial\Omega_d \cup \partial\Omega_n$ and $\partial\Omega_d \cap \partial\Omega_n = \emptyset$.

The initial configuration of the body (see Figure 1) is denoted $\Omega_0 \in \mathbb{R}^d$ with respective Dirichlet and Neumann boundaries $\partial\Omega_D$ and $\partial\Omega_N$. The transformation mapping $\boldsymbol{\Phi}$ takes a point $\boldsymbol{X} \in \Omega_0$ to $\boldsymbol{x} \in \Omega$, such that $\boldsymbol{x} = \boldsymbol{\Phi}(\boldsymbol{X}) =$

$\boldsymbol{X} + \boldsymbol{u}(\boldsymbol{X})$ where $\boldsymbol{u}$ denotes the displacement of the physical point. Let $\underset{\sim}{\boldsymbol{F}} = \nabla_X \boldsymbol{\Phi} = \underset{\sim}{\boldsymbol{1}} + \nabla_X \boldsymbol{u}$ the transformation gradient. The mechanical problem to solve reads, find $\boldsymbol{u}$ such that:

$$\underset{\sim}{\boldsymbol{F}} - \nabla_X \boldsymbol{u} = \underset{\sim}{\boldsymbol{1}} \quad \text{in } \Omega_0 \tag{1a}$$

$$\underset{\sim}{\boldsymbol{P}} - \frac{\partial \psi_{\Omega_0}}{\partial \underset{\sim}{\boldsymbol{F}}} = 0 \quad \text{in } \Omega_0 \tag{1b}$$

$$\nabla_X \cdot \underset{\sim}{\boldsymbol{P}} - \boldsymbol{f}_V = 0 \quad \text{in } \Omega_0 \tag{1c}$$

$$\boldsymbol{u} = \boldsymbol{u}_D \quad \text{on } \partial_D \Omega_0 \tag{1d}$$

$$\underset{\sim}{\boldsymbol{P}} \cdot \boldsymbol{n} = \boldsymbol{t}_N \quad \text{on } \partial_N \Omega_0 \tag{1e}$$

where ψ_{Ω_0} denotes the mechanical energy potential of the body Ω_0, and $\underset{\sim}{\boldsymbol{P}}$ is the first Piola-Kirchoff stress tensor.

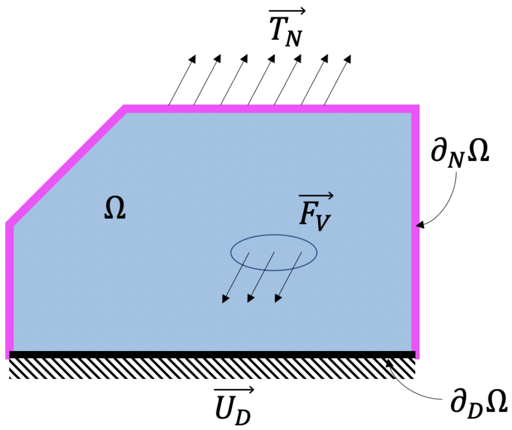

Figure 1. schematic representation of the model problem

The equilibrium of the body Ω_0 is reached for the displacement field $\boldsymbol{u} \in H^1(\Omega_0, \mathbb{R}^d)$ minimizing the energy functional:

$$J_{\Omega_0}(\boldsymbol{u}) = \int_{\Omega_0} \psi_{\Omega_0} - \int_{\Omega_0} \boldsymbol{f}_V \cdot \boldsymbol{u} - \int_{\partial_N \Omega_0} \boldsymbol{t}_N \cdot \boldsymbol{u} \tag{2}$$

corresponding to problem (1) where equations (1a) and (1b) are enforced strongly. If (1a) and (1b) are considered in weak sense, one obtains the three-field Hu–Washizu functional :

$$J_{\Omega_0}(\boldsymbol{u}, \underset{\sim}{\boldsymbol{G}}, \underset{\sim}{\boldsymbol{P}}) = \int_{\Omega_0} \psi_{\Omega_0} + (\nabla_X \boldsymbol{u} - \underset{\sim}{\boldsymbol{G}}) : \underset{\sim}{\boldsymbol{P}} - \int_{\Omega_0} \boldsymbol{f}_V \cdot \boldsymbol{u} - \int_{\partial_N \Omega_0} \boldsymbol{t}_N \cdot \boldsymbol{u} \tag{3}$$

where $\underset{\sim}{\boldsymbol{P}} \in H^1_{\mathrm{div}}(\Omega_0, \mathbb{R}^{d\times d})$, $\underset{\sim}{\boldsymbol{F}} \in L^2(\Omega_0, \mathbb{R}^{d\times d})$, and $\underset{\sim}{\boldsymbol{G}} := \underset{\sim}{\boldsymbol{F}} - \underset{\sim}{\boldsymbol{1}} \in L^2(\Omega_0, \mathbb{R}^{d\times d})$.

2.2. Hybrid mesh

Since the Hybird High Order method relies on both cell and faces unknowns, a so called hybrid mesh is considered. It consists in a collection of cells, as is the case with the standard Finite Element method, and in the collection of the cell faces, forming the skeleton of the mesh. Hence, let $\mathcal{T}_h(\Omega_0)$ the cell collection be a triangulation of the domain Ω_0 into a set of disjoints open polyhedra with planar faces called elements (or cells) $T_i \subset \mathbb{R}^d, 1 \leq i \leq N_T$, where N_T denotes the number of elements in the mesh, such that $\Omega_0 = \cup_{1\leq i\leq N_T} T_i$. For each element T_i, let $\partial T_i \subset \mathbb{R}^{d-1}$ its boundary, composed of its faces (if $d = 3$) or edges (if $d = 2$).

Let $\mathcal{F}_h(\Omega_0)$ the skeleton of the mesh, collecting all element faces in the mesh. A face $F \subset \mathbb{R}^{d-1}$ is a closed subset of Ω_0, and either there are two cells T_1 and T_2 such that $F = \partial T_1 \cap \partial T_2$ (F is then an interior face), or there is a single cell T such that $F = \partial T \cap \partial \Omega_0$ (F is then an exterior face).

Let $\mathcal{F}_h^i(\Omega_0)$ denote the set of interior faces, and $\mathcal{F}_h^e(\Omega_0)$ that of exterior ones. $\mathcal{F}_h^e(\Omega_0)$ is partitioned into $\mathcal{F}_{h,D}^e(\Omega_0) = \{F \in \mathcal{F}_h^e(\Omega_0) \mid F \subset \partial_D\Omega_0\}$ the set of exterior faces imposed to prescribed Dirichlet boundary conditions, and into $\mathcal{F}_{h,N}^e(\Omega_0) = \{F \in \mathcal{F}_h^e(\Omega_0) \mid F \subset \partial_N\Omega_0\}$ the set of exterior faces imposed to prescribed Neumann boundary conditions.

2.3. Introducing

Since the cell displacement field is discontinuous on the mesh, it is sought in the so called broken Sobolev space $H^1(\mathcal{T}_h(\Omega_0), \mathbb{R}^d) = \{\boldsymbol{v} \in L^2(\Omega_0, \mathbb{R}^d) \mid \boldsymbol{v}_T \in H^1(T, \mathbb{R}^d), \forall T \in \mathcal{T}_h(\Omega_0)\}$. In addition, the face displacement field over the mesh is sought in $L^2(\mathcal{F}_h(\Omega_0), \mathbb{R}^d) = \{\boldsymbol{v} \in L^2(\partial T, \mathbb{R}^d), \forall T \in \mathcal{T}_h(\Omega_0)\}$, such that the global displacement field is in $U = H^1(\mathcal{T}_h(\Omega_0), \mathbb{R}^d) \times L^2(\mathcal{F}_h(\Omega_0), \mathbb{R}^d)$

2.4. Composite Element

In order to introduce the discontinuous setting in which lies the Hybrid High Order method, let consider a mesh composed of composite elements, each formed by a bulk part and an interface part between the bulk and the faces of the element, of width some characteristic length. The aim of this section consists in expressing the mechanical equilibrium of such a composite element in order to introduce the main operatos at the foundation of discontinous methods, and in meeting the discontinuous setting by making the characteristic length tend towards zero.

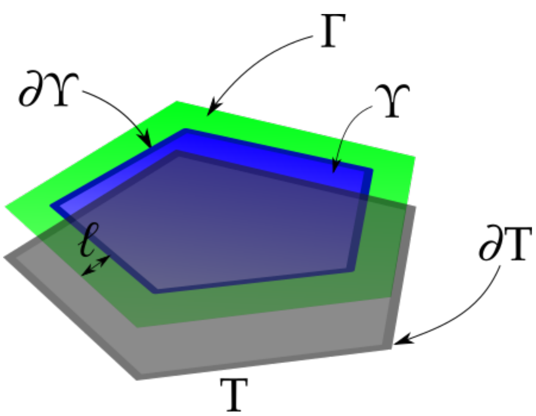

2.4.1. Composite element geometry

Let consider an element T, an open subset of $\mathbb{R}^d$, with boundary ∂T, split into a thin open volumic region $\Gamma \subset T$ of width $\ell > 0$, called the interface, that is attached to the element boundary ∂T, and into an open bulk region $\Upsilon \subset T$, such that

$$\Upsilon \cup \Gamma = T \quad \text{and} \quad \overline{\Upsilon} \cap \overline{\Gamma} = \partial\Upsilon$$

where $\partial\Upsilon$ denotes the boundary of Υ. Let $\boldsymbol{\Phi}_T$ the homotethy of ratio $(1 + \alpha\ell)$ and center $\boldsymbol{X}_T$ the centroid of T, with $\alpha < 0$ such that Υ (respectively $\partial\Upsilon$) is the image of T (respectively ∂T) by $\boldsymbol{\Phi}_T$. Since $\partial\Upsilon$ is an homotethy of ∂T, any point $\boldsymbol{X}_{\partial T} \in \partial T$ and $\boldsymbol{X}_{\partial\Upsilon} = \boldsymbol{\Phi}_T(\boldsymbol{X}_{\partial T}) \in \partial\Upsilon$ share the same unit outward normal $\boldsymbol{n}$. Furthermore, let introduce the following property for integrable functions in Γ:

Property 2.1. *Let $C_\Gamma = \{v \in L^2(\Gamma) \mid v \cdot \boldsymbol{n} = cste\}$ the set of L^2-functions which are constant along the normal axis in Γ. For any function in C_Γ, the following equality holds true:*

$$\int_\Gamma v \, dV = \int_{\partial T} \int_{\epsilon=0}^{\ell} v(1 + \alpha\epsilon) \, dS \, d\epsilon = \ell(1 + \frac{\alpha}{2}\ell) \int_{\partial T} v \, dS \tag{4}$$

2.4.2. Composite element behaviour

Let endow the bulk volume Υ with a displacement field $\boldsymbol{u}_\Upsilon$, such that it is *a priori* free to move independently from the boudary ∂T, with a displacement field $\boldsymbol{u}_{\partial T}$. In order to ensure continuity of the displacement and to bind the displacement of Υ to that of ∂T, let Γ act as a patch between Υ and ∂T, such that $\boldsymbol{u}_\Gamma$ the displacement of Γ links that of Υ to that of ∂T. Furthermore, assuming the interface Γ to be thin compared to the cell volume T, such that $\ell \ll h_T$ is negligeable with respect to h_T the diameter of T, let linearize the displacement in Γ with respect to $\boldsymbol{n}$, such that :

$$\boldsymbol{u}_\Gamma = \frac{\boldsymbol{u}_{\partial T} - \boldsymbol{u}_\Upsilon|_{\partial\Upsilon}}{\ell} \otimes \boldsymbol{n} \cdot \boldsymbol{X} + \boldsymbol{u}_\Upsilon|_{\partial\Upsilon} \tag{5}$$

Let $\psi_\Upsilon = \psi_{\Omega_0}$ the free energy potential in the bulk Υ and ψ_Γ that in Γ. The interface Γ is supposed to behave like a linear elsatic material with a Young modulus β and a zero Poisson ratio, such that :

$$\psi_\Gamma = \frac{1}{2}\beta\frac{\ell}{h_T}\nabla_X \boldsymbol{u}_\Gamma : \nabla_X \boldsymbol{u}_\Gamma \tag{6}$$

where the dimensionless ratio ℓ/h_T balances the accumulated energy with the size of the element. Thus, the element T is made out of a composite material, with a linear elastic layer Γ and a bulk (or matrix) layer Υ with respective behaviours ψ_Γ and ψ_{Ω_0}. Let $\underset{\sim}{\boldsymbol{P}}_\Upsilon$ the first Piola Kirchoff stress tensor in the bulk Υ, and let $\underset{\sim}{\boldsymbol{P}}_\Gamma$ that in Γ. Since Γ is thin compared to Υ, let suppose that the stress in Γ is homogeneous along $\boldsymbol{n}$, such that it carries the traction force from the boundary $\partial\Upsilon$ to ∂T. By continuity of the traction force across $\partial\Upsilon$, the following equality holds true :

$$(\underset{\sim}{\boldsymbol{P}}_\Gamma - \underset{\sim}{\boldsymbol{P}}_\Upsilon|_{\partial\Upsilon}) \cdot \boldsymbol{n} = 0 \tag{7}$$

Let $\boldsymbol{u}_T, \psi_T, \underset{\sim}{\boldsymbol{P}}_T$ respectively the displacement, the free energy potential and the stress in T such that :

$$\boldsymbol{u}_T = \begin{cases} \boldsymbol{u}_\Upsilon & \text{in } \Upsilon \\ \boldsymbol{u}_\Gamma & \text{in } \Gamma \end{cases} \quad , \quad \psi_T = \begin{cases} \psi_\Upsilon & \text{in } \Upsilon \\ \psi_\Gamma & \text{in } \Gamma \end{cases} \quad , \quad \underset{\sim}{\boldsymbol{P}}_T = \begin{cases} \underset{\sim}{\boldsymbol{P}}_\Upsilon & \text{in } \Upsilon \\ \underset{\sim}{\boldsymbol{P}}_\Gamma & \text{in } \Gamma \end{cases} \tag{8}$$

2.5. Element enregy balance

Following (3) and writing J_T the Hu–Washizu functional over the composite element T yields :

$$J_T = \int_\Upsilon \psi_\Upsilon + (\nabla_X \boldsymbol{u}_\Upsilon - \underset{\sim}{\boldsymbol{G}}_\Upsilon) : \underset{\sim}{\boldsymbol{P}}_\Upsilon + \int_\Gamma \psi_\Gamma + (\nabla_X \boldsymbol{u}_\Gamma - \underset{\sim}{\boldsymbol{G}}_\Gamma) : \underset{\sim}{\boldsymbol{P}}_\Gamma - \int_\Upsilon \boldsymbol{f}_V \cdot \boldsymbol{u}_\Upsilon - \int_{\partial_N T} \boldsymbol{t}_{\partial T} \cdot \boldsymbol{u}_{\partial T} \tag{9}$$

where $\underset{\sim}{\boldsymbol{G}}_\Upsilon$ and $\underset{\sim}{\boldsymbol{G}}_\Gamma$ are the displacement gradient unknowns in respectively Υ and Γ. $\boldsymbol{t}_{\partial T}$ denotes the resulting contact forces applied on ∂T, *i.e.* it is either equal to $\boldsymbol{t}_N$ if $\partial T \subset \partial_N \Omega_0$, or to $\boldsymbol{t}_{T' \to T}$ the contatc force applyed by T' to T for any neighbouring element T' sharing a boundary with T. In particular, we assumed that the volumetric load is concentrated in the core part of the element Υ, and neglegted in the boundary part. Using (5) and (4) for $\psi_\Gamma \in C_\Gamma$ one can write the expression of the mechanical energy in the membrane as a term only depending on the boundary :

$$\int_\Gamma \psi_\Gamma = (1 + \frac{\alpha}{2}\ell) \int_{\partial T} \frac{\beta}{2h_T} ||\boldsymbol{u}_{\partial T} - \boldsymbol{u}_\Upsilon|_{\partial\Upsilon}||^2 \tag{10}$$

using a similar argument for the second volumetric term, as well as (7) one has:

$$\int_\Gamma (\nabla_X \boldsymbol{u}_\Gamma - \underset{\sim}{\boldsymbol{G}}_\Gamma) : \underset{\sim}{\boldsymbol{P}}_\Gamma = (1 + \frac{\alpha}{2}\ell) \int_{\partial T} (\boldsymbol{u}_{\partial T} - \boldsymbol{u}_\Upsilon|_{\partial\Upsilon}) \otimes \boldsymbol{n} : \underset{\sim}{\boldsymbol{P}}_\Upsilon|_{\partial\Upsilon} - \int_\Gamma \underset{\sim}{\boldsymbol{G}}_\Gamma : \underset{\sim}{\boldsymbol{P}}_\Gamma \tag{11}$$

using (11) and (10) in the expression of J_T yields:

$$\begin{aligned} J_T = &\int_\Upsilon \psi_\Upsilon + (\nabla_X \boldsymbol{u}_\Upsilon - \underset{\sim}{\boldsymbol{G}}_\Upsilon) : \underset{\sim}{\boldsymbol{P}}_\Upsilon + (1 + \frac{\alpha}{2}\ell) \int_{\partial T} (\boldsymbol{u}_{\partial T} - \boldsymbol{u}_T|_{\partial T}) \otimes \boldsymbol{n} : \underset{\sim}{\boldsymbol{P}}_\Upsilon|_{\partial\Upsilon} \\ &+ (1 + \frac{\alpha}{2}\ell) \int_{\partial T} \frac{\beta}{2h_T} ||\boldsymbol{u}_{\partial T} - \boldsymbol{u}_\Upsilon|_{\partial\Upsilon}||^2 - \int_\Gamma \underset{\sim}{\boldsymbol{G}}_\Gamma : \underset{\sim}{\boldsymbol{P}}_\Gamma - \int_\Upsilon \boldsymbol{f}_V \cdot \boldsymbol{u}_\Upsilon - \int_{\partial_N T} \boldsymbol{t}_{\partial T} \cdot \boldsymbol{u}_{\partial T} \end{aligned} \tag{12}$$

Since ℓ is arbitrary, let $\ell \to 0$; the interface region vanishes such that $\Gamma \to \emptyset, \Upsilon \to T$ and $\partial\Upsilon \to \partial T$. Using a density argument, one has $\boldsymbol{u}_\Upsilon = \boldsymbol{u}_T, \psi_\Upsilon = \psi_T$ and $\underset{\sim}{\boldsymbol{P}}_\Upsilon = \underset{\sim}{\boldsymbol{P}}_T$, and the expression of the Hu–Washizu functional over the element T writes:

$$\begin{aligned} J_T = &\int_T \psi_T + (\nabla_X \boldsymbol{u}_T - \underset{\sim}{\boldsymbol{G}}_T) : \underset{\sim}{\boldsymbol{P}}_T + \int_{\partial T} (\boldsymbol{u}_{\partial T} - \boldsymbol{u}_T|_{\partial T}) \otimes \boldsymbol{n} : \underset{\sim}{\boldsymbol{P}}_T|_{\partial T} + \int_{\partial T} \frac{\beta}{2h_T} \|\boldsymbol{u}_{\partial T} - \boldsymbol{u}_T|_{\partial T}\|^2 \\ &- \int_T \boldsymbol{f}_V \cdot \boldsymbol{u}_T - \int_{\partial_N T} \boldsymbol{t}_{\partial T} \cdot \boldsymbol{u}_{\partial T} \end{aligned} \tag{13}$$

Assuming that the displacement is continuous at the boundary ∂T such that $\boldsymbol{u}_{\partial T} - \boldsymbol{u}_T|_{\partial T} = 0$ one recovers the usual expression of the Hu–Washizu integral over the element for the three variables $(\boldsymbol{u}_T, \underset{\sim}{\boldsymbol{G}}_T, \underset{\sim}{\boldsymbol{P}}_T)$. However, if one considers that $\boldsymbol{u}_{\partial T}$ and $\boldsymbol{u}_T$ are disticnt variables, *i.e.* that the displacement across ∂T is discontinuous, the functional writes as a function of the four variables $(\boldsymbol{u}_T, \boldsymbol{u}_{\partial T}, \underset{\sim}{\boldsymbol{G}}_T, \underset{\sim}{\boldsymbol{P}}_T)$. Differentiating J_T over each of these variables, and introducing the numerical flux $\boldsymbol{\theta}_{\partial T} = \underset{\sim}{\boldsymbol{P}}_T|_{\partial T} \cdot \boldsymbol{n} + (\beta/h_T)(\boldsymbol{u}_{\partial T} - \boldsymbol{u}_T|_{\partial T})$ one obtains the system:

$$\frac{\partial J_T}{\partial \boldsymbol{u}_T}\delta \boldsymbol{u}_T = \int_T (\underset{\sim}{\boldsymbol{P}}_T : \nabla_X \delta \boldsymbol{u}_T - \boldsymbol{f}_V) \cdot \delta \boldsymbol{u}_T - \int_{\partial T} \boldsymbol{\theta}_{\partial T} \cdot \delta \boldsymbol{u}_T|_{\partial T} \qquad \forall \delta \boldsymbol{u}_T \tag{14a}$$

$$\frac{\partial J_T}{\partial \boldsymbol{u}_{\partial T}}\delta \boldsymbol{u}_{\partial T} = \int_{\partial T} (\boldsymbol{\theta}_{\partial T} - \boldsymbol{t}_N) \cdot \delta \boldsymbol{u}_{\partial T} \qquad \forall \delta \boldsymbol{u}_{\partial T} \tag{14b}$$

$$\frac{\partial J_T}{\partial \underset{\sim}{\boldsymbol{G}}_T}\delta \underset{\sim}{\boldsymbol{G}}_T = \int_T (\frac{\partial \psi_T}{\partial \underset{\sim}{\boldsymbol{G}}_T} - \underset{\sim}{\boldsymbol{P}}_T) : \delta \underset{\sim}{\boldsymbol{G}}_T \qquad \forall \delta \underset{\sim}{\boldsymbol{G}}_T \tag{14c}$$

$$\frac{\partial J_T}{\partial \underset{\sim}{\boldsymbol{P}}_T}\delta \underset{\sim}{\boldsymbol{P}}_T = \int_T (\nabla_X \boldsymbol{u}_T - \underset{\sim}{\boldsymbol{G}}_T) : \delta \underset{\sim}{\boldsymbol{P}}_T + \int_{\partial T} (\boldsymbol{u}_{\partial T} - \boldsymbol{u}_T|_{\partial T}) \otimes \boldsymbol{n} : \delta \underset{\sim}{\boldsymbol{P}}_T|_{\partial T} \qquad \forall \delta \underset{\sim}{\boldsymbol{P}}_T \tag{14d}$$

By explicitly eliminating (14c) and (14d) from the system, one obtains the problem in primal form: find $(\boldsymbol{u}_T, \boldsymbol{u}_{\partial T})$, such that for all $(\delta \boldsymbol{u}_T, \delta \boldsymbol{u}_{\partial T})$

$$dJ_T = \frac{\partial J_T}{\partial \boldsymbol{u}_T}\delta \boldsymbol{u}_T + \frac{\partial J_T}{\partial \boldsymbol{u}_{\partial T}}\delta \boldsymbol{u}_{\partial T} = 0 \tag{15}$$

injetcing (14a) and (14b) :

$$\begin{aligned} dJ_T = &\int_T \underset{\sim}{\boldsymbol{P}}_T : \nabla_X \delta \boldsymbol{u}_T + \int_{\partial T} (\delta \boldsymbol{u}_{\partial T} - \delta \boldsymbol{u}_T|_{\partial T}) \otimes \boldsymbol{n} : \underset{\sim}{\boldsymbol{P}}_T|_{\partial T} + \int_{\partial T} (\beta/h_T)(\boldsymbol{u}_{\partial T} - \boldsymbol{u}_T|_{\partial T}) \cdot (\delta \boldsymbol{u}_{\partial T} - \delta \boldsymbol{u}_T|_{\partial T}) \\ &- \int_{\partial T} \boldsymbol{t}_N \cdot \delta \boldsymbol{u}_{\partial T} - \int_T \boldsymbol{f}_V \cdot \delta \boldsymbol{u}_T \end{aligned} \tag{16}$$

using both (14c) and (14d) :

$$dJ_T = \int_T \frac{\partial \psi_T}{\partial \underset{\sim}{\boldsymbol{G}}_T} : \delta \underset{\sim}{\boldsymbol{G}}_T + \int_{\partial T} (\beta/h_T)(\boldsymbol{u}_{\partial T} - \boldsymbol{u}_T|_{\partial T}) \cdot (\delta \boldsymbol{u}_{\partial T} - \delta \boldsymbol{u}_T|_{\partial T}) - \int_{\partial T} \boldsymbol{t}_N \cdot \delta \boldsymbol{u}_{\partial T} - \int_T \boldsymbol{f}_V \cdot \delta \boldsymbol{u}_T \tag{17}$$

where $\delta \underset{\sim}{\boldsymbol{G}}_T$ (respectively $\underset{\sim}{\boldsymbol{G}}_T$) solves (14d) for the unknowns set $(\delta \boldsymbol{u}_T, \delta \boldsymbol{u}_{\partial T})$ (respectively $(\boldsymbol{u}_T, \boldsymbol{u}_{\partial T})$)

2.6. Discretization

Problem (17) describes the continuous problem. The discrete problem consists in seeking the unknown couple $(\boldsymbol{u}_T, \boldsymbol{u}_{\partial T})$ in a .

Le problème (**??**) discrétisé consiste à chercher l'inconnue $(\boldsymbol{u}_T^l, \boldsymbol{u}_{\partial T}^k)$ dans l'espace des polynômes $P^l(T, \mathbb{R}^d) \times P^k(\partial T, \mathbb{R}^d)$ d'ordre respectivement l et k tels que $k > 0$ avec $k-1 \le l \le k+1$, et les champs de gradients de déplacement $\underset{\sim}{\boldsymbol{G}}_T^k$ et de contraintes $\underset{\sim}{\boldsymbol{P}}_T^k$ dans $P^k(T, \mathbb{R}^{d \times d})$. On définit la force de traction discrète $\boldsymbol{\theta}_{\partial T}^{HHO} = \underset{\sim}{\boldsymbol{P}}_T^k \cdot \boldsymbol{n} + (\beta_{mec}/h_T)\boldsymbol{S}_{\partial T}^{k*}$ telle que $\boldsymbol{S}_{\partial T}^{k*}$ est l'opérateur adjoint de l'opérateur de stabilisation $\boldsymbol{S}_{\partial T}^k$ définit par:

$$\boldsymbol{S}_{\partial T}^k(\boldsymbol{v}_T^l, \boldsymbol{v}_{\partial T}^k) = \Pi_{\partial T}^k(\boldsymbol{v}_{\partial T}^k - \boldsymbol{v}_T^l - (\boldsymbol{1} - \Pi_T^k)\boldsymbol{D}_T^{k+1}) \tag{18}$$

où $\Pi^k_{\partial T}$ et Π^k_T sont les projecteurs orthogonaux au sens L^2 sur $P^k(\partial T, \mathbb{R}^d)$ et $P^k(T, \mathbb{R}^d)$ respectivement, et le champ de déplacement $\boldsymbol{D}^{k+1}_T \in P^{k+1}(T, \mathbb{R}^d)$ est solution du problème (19):

$$\begin{aligned} \int_T (\nabla_X \boldsymbol{D}^{k+1}_T - \nabla_X \boldsymbol{u}^l_T) : \nabla_X \boldsymbol{w}^{k+1} &= \int_{\partial T} (\boldsymbol{u}^k_{\partial T} - \boldsymbol{u}^l_T) \cdot \nabla_X \boldsymbol{w}^{k+1} \boldsymbol{n} \quad \forall \boldsymbol{w}^{k+1} \in P^{k+1}(T, \mathbb{R}^d) \\ \int_T \boldsymbol{D}^{k+1}_T &= \int_T \boldsymbol{u}^l_T \end{aligned} \tag{19}$$

D'un point de vue numérique, on calcule dans une étape de pré-traitement l'opérateur de stabilisation $[S] : (\boldsymbol{v}^l_T, \boldsymbol{v}^k_{\partial T}) \to \boldsymbol{S}^k_{\partial T}$ défini par (18) et l'opérateur de dérivation $[B] : (\boldsymbol{v}^l_T, \boldsymbol{v}^k_{\partial T}) \to \underset{\sim}{\boldsymbol{G}}^k_T$ défini par la formulation discrète de (**??**), de sorte que le problème discrétisé local (**??**) ne dépend plus que de l'inconnue primale $(\boldsymbol{u}^l_T, \boldsymbol{u}^k_{\partial T})$ vérifiant $\forall(\boldsymbol{v}^l_T, \boldsymbol{v}^k_{\partial T}) \in P^l(T, \mathbb{R}^d) \times P^k(\partial T, \mathbb{R}^d)$:

$$\int_T \underset{\sim}{\boldsymbol{P}}^k_T : \underset{\sim}{\boldsymbol{G}}^k_T + \int_{\partial_T} \frac{\beta_{mec}}{h_T} \boldsymbol{S}^k_{\partial T}(\boldsymbol{u}^l_T, \boldsymbol{u}^k_{\partial T}) \cdot \boldsymbol{S}^k_{\partial T}(\boldsymbol{v}^l_T, \boldsymbol{v}^k_{\partial T}) = \int_\Omega \boldsymbol{f}_V \cdot \boldsymbol{v}^l_T + \int_{\partial_T} \boldsymbol{t}_N \cdot \boldsymbol{v}^k_{\partial T} \tag{20}$$

où les contraintes $\underset{\sim}{\boldsymbol{P}}^k_T$ sont calculées aux points de quadrature par intégration de la loi de comportement. Le principe des travaux virtuels discret à l'échelle de la structure vérifie donc $\forall(\boldsymbol{v}^l_{\mathcal{T}}, \boldsymbol{v}^k_{\mathcal{F}}) \in P^l(\mathcal{T}, \mathbb{R}^d) \times P^k(\mathcal{F}, \mathbb{R}^d)$:

$$\begin{aligned} \sum_{T \in \mathcal{T}(\Omega_0)} \int_T \underset{\sim}{\boldsymbol{P}}^k_T : \underset{\sim}{\boldsymbol{G}}^k_T + \int_{\partial_T} \frac{\beta_{mec}}{h_T} \boldsymbol{S}^k_{\partial T}(\boldsymbol{u}^l_T, \boldsymbol{u}^k_{\partial T}) \cdot \boldsymbol{S}^k_{\partial T}(\boldsymbol{v}^l_T, \boldsymbol{v}^k_{\partial T}) = &\sum_{T \in \mathcal{T}(\Omega_0)} \int_\Omega \boldsymbol{f}_V \cdot \boldsymbol{v}^l_T \\ &+ \sum_{\partial T \in \mathcal{F}_N(\Omega_0)} \int_{\partial_T} \boldsymbol{t}_N \cdot \boldsymbol{v}^k_{\partial T} \end{aligned} \tag{21}$$

References

[1] W. Reed, T. Hill, Triangular mesh methods for the neutron transport equation, Tech. rep., United States, lA-UR–73-479 INIS Reference Number: 4080130 (1973).

[2] I. Babuska, The Finite Element Method with Penalty, Mathematics of Computation 27 (122) (1973) 221. doi:10.2307/2005611.
URL https://www.jstor.org/stable/2005611?origin=crossref

[3] V. J. Nitsche, Uber ein Yariationsprinzip zur Liisung yon Dirichlet-Problemen bei Verwendung yon Teilr¯iumen, die keinen Randbedingungen unterworfen sind (1970) 7.

[4] P. Hansbo, M. G. Larson, Discontinuous Galerkin methods for incompressible and nearly incompressible elasticity by Nitsche's method, Computer Methods in Applied Mechanics and Engineering 191 (17-18) (2002) 1895–1908. doi:10.1016/S0045-7825(01)00358-9.
URL https://linkinghub.elsevier.com/retrieve/pii/S0045782501003589

[5] M. F. Wheeler, An Elliptic Collocation-Finite Element Method with Interior Penalties, SIAM Journal on Numerical Analysis 15 (1) (1978) 152–161. doi:10.1137/0715010.
URL http://epubs.siam.org/doi/10.1137/0715010

[6] B. Rivière, M. F. Wheeler, Optimal Error Estimates for Discontinuous Galerkin Methods Applied to Linear Elasticity Problems, Comput. Math. Appl 46 (2000) 141–163.

[7] A. Lew, P. Neff, D. Sulsky, M. Ortiz, Optimal BV estimates for a discontinuous Galerkin method for linear elasticity, Applied Mathematics Research eXpress 2004 (3) (2004) 73. doi:10.1155/S1687120004020052.
URL https://academic.oup.com/amrx/article-lookup/doi/10.1155/S1687120004020052

[8] F. Celiker, B. Cockburn, H. K. Stolarski, Locking-Free Optimal Discontinuous Galerkin Methods for Timoshenko Beams, SIAM Journal on Numerical Analysis 44 (6) (2006) 2297–2325.
URL http://www.jstor.org/stable/40232896

[9] S. C. Brenner, L.-y. Sung, Balancing domain decomposition for nonconforming plate elements, Numerische Mathematik 83 (1) (1999) 25–52. doi:10.1007/s002110050438.
URL https://doi.org/10.1007/s002110050438

[10] G. Engel, K. Garikipati, T. Hughes, M. Larson, L. Mazzei, R. Taylor, Continuous/discontinuous finite element approximations of fourth-order elliptic problems in structural and continuum mechanics with applications to thin beams and plates, and strain gradient elasticity, Computer Methods in Applied Mechanics and Engineering 191 (34) (2002) 3669–3750. doi:10.1016/S0045-7825(02)00286-4.
URL https://linkinghub.elsevier.com/retrieve/pii/S0045782502002864

[11] D. N. Arnold, F. Brezzi, L. D. Marini, A Family of Discontinuous Galerkin Finite Elements for the Reissner–Mindlin Plate, Journal of Scientific Computing 22 (1) (2005) 25–45. doi:10.1007/s10915-004-4134-8.
URL https://doi.org/10.1007/s10915-004-4134-8

[12] A. Ten Eyck, A. Lew, Discontinuous Galerkin methods for non-linear elasticity, International Journal for Numerical Methods in Engineering 67 (9) (2006) 1204–1243. doi:10.1002/nme.1667.
URL https://onlinelibrary.wiley.com/doi/10.1002/nme.1667

[13] L. Noels, R. Radovitzky, A general discontinuous Galerkin method for finite hyperelasticity. Formulation and numerical applications, International Journal for Numerical Methods in Engineering 68 (1) (2006) 64–97. doi:10.1002/nme.1699.
URL https://onlinelibrary.wiley.com/doi/10.1002/nme.1699

[14] C. Ortner, E. Süli, Discontinuous Galerkin Finite Element Approximation of Nonlinear Second-Order Elliptic and Hyperbolic Systems, SIAM Journal on Numerical Analysis 45 (4) (2007) 1370–1397, publisher: Society for Industrial and Applied Mathematics. doi:10.1137/06067119X.
URL https://epubs.siam.org/doi/10.1137/06067119X

[15] K. Shahbazi, P. F. Fischer, C. R. Ethier, A high-order discontinuous Galerkin method for the unsteady incompressible Navier–Stokes equations, Journal of Computational Physics 222 (1) (2007) 391–407. doi:10.1016/j.jcp.2006.07.029.
URL https://linkinghub.elsevier.com/retrieve/pii/S0021999106003585

[16] P.-O. Persson, J. Bonet, J. Peraire, Discontinuous Galerkin solution of the Navier–Stokes equations on deformable domains, Computer Methods in Applied Mechanics and Engineering 198 (17-20) (2009) 1585–1595. doi:10.1016/j.cma.2009.01.012.
URL https://linkinghub.elsevier.com/retrieve/pii/S0045782509000450

[17] R. Gracie, H. Wang, T. Belytschko, Blending in the extended finite element method by discontinuous Galerkin and assumed strain methods, International Journal for Numerical Methods in Engineering 74 (11) (2008) 1645–1669, _eprint: https://onlinelibrary.wiley.com/doi/pdf/10.1002/nme.2217. doi:10.1002/nme.2217.
URL https://onlinelibrary.wiley.com/doi/abs/10.1002/nme.2217

[18] Y. Shen, A. Lew, Stability and convergence proofs for a discontinuous-Galerkin-based extended finite element method for fracture mechanics, Computer Methods in Applied Mechanics and Engineering 199 (37) (2010) 2360–2382. doi:10.1016/j.cma.2010.03.008.
URL https://www.sciencedirect.com/science/article/pii/S0045782510000848

[19] J. K. Djoko, F. Ebobisse, A. T. McBride, B. D. Reddy, A discontinuous Galerkin formulation for classical and gradient plasticity – Part 1: Formulation and analysis, Computer Methods in Applied Mechanics and Engineering 196 (37) (2007) 3881–3897. doi:10.1016/j.cma.2006.10.045.
URL https://www.sciencedirect.com/science/article/pii/S0045782507001144

[20] J. K. Djoko, F. Ebobisse, A. T. McBride, B. D. Reddy, A discontinuous Galerkin formulation for classical and gradient plasticity. Part 2: Algorithms and numerical analysis, Computer Methods in Applied Mechanics and Engineering 197 (1) (2007) 1–21. doi:10.1016/j.cma.2007.06.027.
URL https://www.sciencedirect.com/science/article/pii/S0045782507002964

[21] B. Cockburn, J. Gopalakrishnan, R. Lazarov, Unified Hybridization of Discontinuous Galerkin, Mixed, and Continuous Galerkin Methods for Second Order Elliptic Problems, SIAM Journal on Numerical Analysis 47 (2) (2009) 1319–1365. doi:10.1137/070706616.
URL http://epubs.siam.org/doi/10.1137/070706616

[22] S.-C. Soon, B. Cockburn, H. K. Stolarski, A hybridizable discontinuous Galerkin method for linear elasticity: AN HDG METHOD, International Journal for Numerical Methods in Engineering 80 (8) (2009) 1058–1092. doi:10.1002/nme.2646.
URL https://onlinelibrary.wiley.com/doi/10.1002/nme.2646

[23] S.-C. Soon, Hybridizable discontinuous Galerkin method for solid mechanics, Ph.D. thesis, University of Minnesota (2008).

[24] N. Nguyen, J. Peraire, B. Cockburn, An implicit high-order hybridizable discontinuous Galerkin method for linear convection–diffusion equations, Journal of Computational Physics 228 (9) (2009) 3232–3254. doi:10.1016/j.jcp.2009.01.030.
URL https://linkinghub.elsevier.com/retrieve/pii/S0021999109000308

[25] N. Nguyen, J. Peraire, B. Cockburn, An implicit high-order hybridizable discontinuous Galerkin method for nonlinear convection–diffusion equations, Journal of Computational Physics 228 (23) (2009) 8841–8855. doi:10.1016/j.jcp.2009.08.030.
URL https://linkinghub.elsevier.com/retrieve/pii/S0021999109004756

[26] N. Nguyen, J. Peraire, B. Cockburn, A hybridizable discontinuous Galerkin method for Stokes flow, Computer Methods in Applied Mechanics and Engineering 199 (9-12) (2010) 582–597. doi:10.1016/j.cma.2009.10.007.
URL https://linkinghub.elsevier.com/retrieve/pii/S0045782509003521

[27] N. Nguyen, J. Peraire, B. Cockburn, An implicit high-order hybridizable discontinuous Galerkin method for the incompressible Navier–Stokes equations, Journal of Computational Physics 230 (4) (2011) 1147–1170. doi:10.1016/j.jcp.2010.10.032.
URL https://linkinghub.elsevier.com/retrieve/pii/S0021999110005887

[28] N. Nguyen, J. Peraire, Hybridizable discontinuous Galerkin methods for partial differential equations in continuum mechanics, Journal of Computational Physics 231 (18) (2012) 5955–5988. doi:10.1016/j.jcp.2012.02.033.
URL https://linkinghub.elsevier.com/retrieve/pii/S0021999112001544

[29] D. A. Di Pietro, A. Ern, A hybrid high-order locking-free method for linear elasticity on general meshes, Computer Methods in Applied Mechanics and Engineering 283 (2015) 1–21. doi:10.1016/j.cma.2014.09.009.
URL https://linkinghub.elsevier.com/retrieve/pii/S0045782514003181

[30] D. A. Di Pietro, A. Ern, S. Lemaire, An Arbitrary-Order and Compact-Stencil Discretization of Diffusion on General Meshes Based on Local Reconstruction Operators, Computational Methods in Applied Mathematics 14 (4) (2014) 461–472. doi:10.1515/cmam-2014-0018.
URL https://www.degruyter.com/document/doi/10.1515/cmam-2014-0018/html

[31] D. A. Di Pietro, A. Ern, A. Linke, F. Schieweck, A discontinuous skeletal method for the viscosity-dependent Stokes problem, Computer Methods in Applied Mechanics and Engineering 306 (2016) 175–195. doi:10.1016/j.cma.2016.03.033.
URL https://linkinghub.elsevier.com/retrieve/pii/S0045782516301189

[32] D. A. Di Pietro, S. Krell, A Hybrid High-Order Method for the Steady Incompressible Navier–Stokes Problem, Journal of Scientific Computing 74 (3) (2018) 1677–1705. doi:10.1007/s10915-017-0512-x.
URL http://link.springer.com/10.1007/s10915-017-0512-x

[33] D. Boffi, M. Botti, D. A. Di Pietro, A Nonconforming High-Order Method for the Biot Problem on General Meshes, SIAM Journal on Scientific Computing 38 (3) (2016) A1508–A1537. doi:10.1137/15M1025505.
URL http://epubs.siam.org/doi/10.1137/15M1025505

[34] M. Botti, D. A. Di Pietro, P. Sochala, A Hybrid High-Order Method for Nonlinear Elasticity, SIAM Journal on Numerical Analysis 55 (6) (2017) 2687–2717. doi:10.1137/16M1105943.
URL https://epubs.siam.org/doi/10.1137/16M1105943